

AD-A187 166

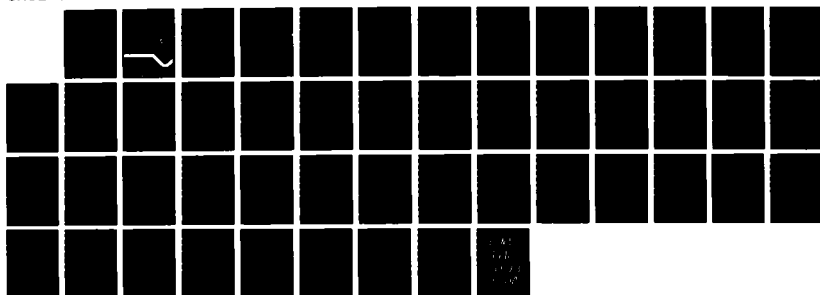
NUCLEAR EXCITATION VIA THE MOTION OF ELECTRONS IN A
STRONG LASER FIELD (U) LAWRENCE LIVERMORE NATIONAL LAB
CA J F BERGER ET AL. JUN 87 UCRL-96759

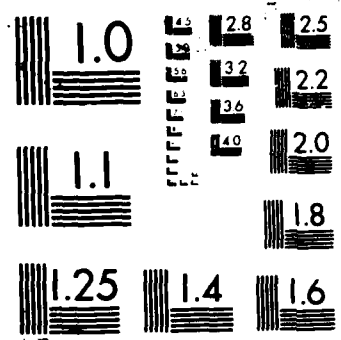
1/1

UNCLASSIFIED

F/G 9/3

NL





AD-A187 166

UCRL-96759
PREPRINT

NUCLEAR EXCITATION VIA THE MOTION OF ELECTRONS
IN A STRONG LASER FIELD

J. F. BERGER
D. GOGNY
M. S. WEISS

THIS PAPER WAS PREPARED FOR SUBMITTAL TO
JOURNAL OF QUANTUM SPECTRUM
AND RADIATION TRANSPORT

DTIC
ELECTE
NOV 12 1987
S
E

JUNE 1987

Lawrence
Livermore
National
Laboratory

This is a preprint of a paper intended for publication in a journal or proceedings. Since changes may be made before publication, this preprint is made available with the understanding that it will not be cited or reproduced without the permission of the author.

This document has been approved
for public release and sale in
distribution is unlimited.

DISCLAIMER

This document was prepared as an account of work sponsored by an agency of the United States Government. Neither the United States Government nor the University of California nor any of their employees, makes any warranty, express or implied, or assumes any legal liability or responsibility for the accuracy, completeness, or usefulness of any information, apparatus, product, or process disclosed, or represents that its use would not infringe privately owned rights. Reference herein to any specific commercial products, process, or service by trade name, trademark, manufacturer, or otherwise, does not necessarily constitute or imply its endorsement, recommendation, or favoring by the United States Government or the University of California. The views and opinions of authors expressed herein do not necessarily state or reflect those of the United States Government or the University of California, and shall not be used for advertising or product endorsement purposes.

J. F. BERGER*, D. GOGNY* and M. S. WEISS**

University of California
Physics Department, Lawrence Livermore National Laboratory
P.O. Box 808, Livermore, California 94550, USA

and

Service PTN, Centre d'Etudes de Bruyères-le-Chatel
BP 12, 91680 Bruyères-le-Chatel, France

NUCLEAR EXCITATION VIA THE MOTION OF
ELECTRONS IN A STRONG LASER FIELD***

ABSTRACT

A method of switching from a nuclear isomeric state to a lasing state is examined. A semi-classical model of laser-electron-nuclear coupling is developed. In it the electrons are treated as free in the external field of the laser, but with initial conditions corresponding to their atomic orbits. Application is made to testing this model in ^{235}U and to the design criteria of a gamma-ray laser.

Submitted to JQSRT

*Permanent Address: Service PTN, Centre d'Etudes de Bruyères-le-Chatel,
BP 12, 91680 Bruyères-le-Chatel, France

**Permanent address: Physics Department, Lawrence Livermore National
Laboratory, P.O. Box 808, Livermore, California 94550, USA

***Supported in part by the Department of Energy at Lawrence Livermore
National Laboratory, Livermore, California, under contract No.
W-7405-Eng-48 and supported in part by SDIO/IST, administered by NRL.

Accession For	
NTIS GRA&I	<input checked="" type="checkbox"/>
DTIC TAB	<input type="checkbox"/>
Unannounced	<input type="checkbox"/>
Justification	
By	
Distribution/	
Availability Codes	
Dist	Avail and/or Special
A-1	

This document has been approved
for public release and sale in
distribution is unlimited.

I. INTRODUCTION

Much effort has been devoted in recent years to the search of physical mechanisms and techniques that would permit the development of a gamma-ray laser.¹ In one of the most promising schemes proposed up to now, energy is first stored in a long-lived (isomeric) nuclear state. Then a fast transition to a short-lived level is induced by some external stimulation. It is presently believed that a certain number of conditions have to be met in order to implement this scenario in practice. In particular, it seems at least desirable that the second step - the lasing phase - populate the upper level of a recoilless Mossbauer-type transition. However, whatever the precise sequence of nuclear levels involved, one basic requirement is to be able to produce a significant population of the storage level, and then switch it to the lasing level in a time shorter than its lifetime.

The purpose of this paper is to analyze the possibilities of a method where the isomer population would be switched to the lasing state by the motion of the atomic electrons in the field of a intense laser. In fact, it seems that highly localized electron current densities can be induced in multi-electron atoms by powerful lasers² and may couple to nuclear excitations.³ A direct excitation of low-lying nuclear levels is therefore conceivable and would be a powerful test of this mechanism. On the other hand, we expect the nuclear transition probability per unit time to be very small since the driven electrons move at average distances from the nucleus comparable to atomic dimensions.

We must emphasize that we have no reason to utilize this method to excite low-lying nuclear states. That is solely a test of the method. If this laser-electron-nucleus coupling has any value, it will be in switching from an

isomeric to a lasing state. We will discuss the conditions in which that could take place later in the paper.

In the present analysis of this problem, we do not attempt to set up a precise description of the laser + electrons + nucleus system. An exact solution is beyond our imagination and a sophisticated approximation (TDHF) is both in progress and very difficult.⁴ Our aim is rather to determine if a laser-electron-nucleus coupling mechanism has any chance at all to be useful for a gamma-ray laser. In this spirit, we develop a very simple model for the electron motion which always errs in overestimating the electron-nucleus coupling, but nevertheless has the structure of a more realistic theory. Namely, we assume that the atomic electrons are set into motion by the electric field of the laser as if they were free. They are hypothesized to move on classical trajectories starting at their location in the atom. The nuclear transition probability derived with these assumptions is therefore an upper limit that is indicative of the possibilities of the method and affords an opportunity to examine these effects as a function of the pertinent parameters. We are free to include or not include individual shells and thus can examine both the effects of atomic binding (relative to the laser energy) and possible coherent electron motion.

As a test case, we choose the $\Delta l=3$ transition from the ground state to the 75 eV, 26 mn isomeric level of ^{235}U which has also been discussed by SOLEM et al.⁵ in a more simplified model which treats the electron cloud as a rigid body. The frequency of this transition being only ~ 15 times that of presently available U-V lasers,⁶ it has been suggested as a very good candidate for testing this mechanism. However, our study extends to more general cases since we determine the dependence of the transition probability

on the frequency and multipolarity of the nuclear transition. We also analyze the influence of the characteristics (frequency and intensity) of the laser.

In the second section we develop our model. The results obtained for the nuclear transition, probability with different sets of parameters, are presented in the third section. In the fourth one, we apply them to the case of ^{235}U . The fifth section details design considerations for a realistic gamma-ray laser with the provision that our calculations underestimate the power and frequency requirements of the mechanism. Conclusions are drawn in the sixth section.

II. MODEL

As mentioned in the introduction, we assume that the effect of the laser is to set into motion all the electrons of the atom as if they were free. In other words, the influence of the Coulomb field of the nucleus as well as the shielding due to the external atomic shells are ignored. In the same spirit, each portion of the electron cloud is supposed to move along a classical trajectory. That is, we choose simplistic initial conditions, namely that each electron is a classical gas whose initial position is governed by its quantum spatial distribution. Neglecting relativistic retardation and re-radiation effects, the motion of the electrons is due entirely to the electric field \vec{E} of the laser. We assume the laser linearly polarized (\vec{E} parallel to \vec{z}) and the wavelength much larger than the atom size (which is true for ultraviolet and soft x-ray lasers). The z-component of the electric field can therefore be written $E_z = E_0 \sin \omega_0 t$ with ω_0 the laser frequency. With these assumptions, each portion of the electron cloud initially located at (x_0, y_0, z_0) acquires a harmonic motion on a linear trajectory:

$$\begin{aligned}
 x_e(t) &= x_0 \\
 y_e(t) &= y_0 \\
 z_e(t) &= z_0 - \gamma \sin \omega_0 t
 \end{aligned}
 \tag{1}$$

with the same amplitude

$$\gamma = \frac{e}{m} \frac{E_0}{\omega_0^2}
 \tag{2}$$

(e and m are the electron charge and mass respectively). Denoting by $\rho_0^{(i)}$ charge distribution of the i-th electron before excitation and by $\rho_t^{(i)}$ its charge distribution when it moves according to (1), we have:

$$\rho_t^{(i)}(\vec{r}_e(t)) = \rho_0^{(i)}(\vec{r}_0)$$

with

$$\vec{r}_e(t) = (x_0, y_0, z_0 - \gamma \sin \omega_0 t) \quad \vec{r}_0 = (x_0, y_0, z_0)$$

The Coulomb field created at point \vec{r} by the i-th moving electron is therefore:

$$\int d^3 r_e(t) \frac{\rho_t^{(i)}(\vec{r}_e(t))}{|\vec{r} - \vec{r}_e(t)|} \equiv \int d^3 r_0 \frac{\rho_0^{(i)}(\vec{r}_0)}{|\vec{r} - \vec{r}_e(t)|}$$

and the time-dependent electron-nucleus interaction is

$$\begin{aligned}
 \hat{V}(t) &= \sum_{i=1}^Z \int d^3 r_0 \rho_0^{(i)}(\vec{r}_0) \times \\
 &\times \sum_{\sigma} \int d^3 r \psi_{\text{prot}}^+(\vec{r}, \sigma) \frac{e^2}{|\vec{r} - \vec{r}_e(t)|} \psi_{\text{prot}}(\vec{r}, \sigma)
 \end{aligned}
 \tag{3}$$

where $\Psi_{\text{prot}}^+(\vec{r}, \sigma)$ (resp. $\Psi_{\text{prot}}(\vec{r}, \sigma)$) is the creation (resp. annihilation) operator of a proton of spin σ at point \vec{r} . The Hamiltonian of the nucleus in the external field created by the Z moving electrons now is

$$\hat{H} = \hat{H}_N + \hat{V}(t)$$

where H_N is the nuclear Hamiltonian, and the time-dependent state $|\phi(t)\rangle$ of the nucleus can be expanded on the eigenstates $|x_n\rangle$ of \hat{H}_N :

$$|\phi(t)\rangle = \sum_n b_n(t) e^{-\frac{i}{\hbar} E_n t} |x_n\rangle$$

$$\hat{H}_N |x_n\rangle = E_n |x_n\rangle$$

We assume the nucleus initially in state $|x_0\rangle$ (with angular momentum I_0).

The probability of finding the nucleus in state $|x_1\rangle$ (with angular momentum I_1) at time T_1 is

$$P(T) = \frac{1}{2I_0 + 1} \sum_{M_0 = -I_0}^{I_0} \sum_{M_1 = -I_1}^{I_1} |b_1(T)|^2 \quad (4)$$

with

$$b_n(T) = \delta_{n,0} + \frac{1}{i\hbar} \int_0^T dt \sum_m \langle x_n | \hat{V}(t) | x_m \rangle e^{\frac{i}{\hbar} (E_n - E_m)t} b_m(t) \quad (5)$$

We first evaluate the nuclear transition probability after one laser cycle of duration $T_0 = 2\pi/\omega_0$. Since T_0 is of the order of $10^{-14} - 10^{-15}$ s and the electron-nucleus interaction is expected to be small, (5) can be evaluated using first order perturbation theory. Then:

$$b_1(T_0) = \frac{1}{i\hbar} \int_0^{T_0} dt \langle x_1 | \hat{V}(t) | x_0 \rangle e^{i\omega_N t} \quad (6)$$

with

$$\omega_N = (E_1 - E_0)/\hbar$$

Inserting the expression (3) of $\hat{V}(t)$ and expanding the Coulomb potential into spherical harmonics gives

$$\begin{aligned} b_1(T_0) = & \sum_{i=1}^Z \int d^3r_0 \rho_0^{(i)}(\vec{r}_0) \sum_{\lambda=0}^{\infty} \sum_{\mu=-\lambda}^{\lambda} \frac{4\pi e^2}{2\lambda+1} \frac{1}{i\hbar} \int_0^{T_0} dt e^{i\omega_N t} Y_{\lambda}^{\mu}(\hat{r}_e(t)) \\ & \times \sum_{\sigma} \int d^2\hat{r} Y_{\lambda}^{\mu*}(\hat{r}) \left(\int_0^{r_e(t)} r^2 dr \frac{r^{\lambda}}{[r_e(t)]^{\lambda+1}} \langle x_1 | \Psi_{\text{prot}}^+(\vec{r}, \sigma) \Psi_{\text{prot}}(\vec{r}, \sigma) | x_0 \rangle \right. \\ & \left. + \int_{r_e(t)}^{\infty} r^2 dr \frac{[r_e(t)]^{\lambda}}{r^{\lambda+1}} \langle x_1 | \Psi_{\text{prot}}^+(\vec{r}, \sigma) \Psi_{\text{prot}}(\vec{r}, \sigma) | x_0 \rangle \right) \quad (7) \end{aligned}$$

We now assume that the nuclear transition matrix element

$$\langle x_1 | \Psi_{\text{prot}}^+(\vec{r}, \sigma) \Psi_{\text{prot}}(\vec{r}, \sigma) | x_0 \rangle$$

is peaked around the nuclear surface. This is certainly valid for transitions between low-lying nuclear states since they involve essentially single-particle or surface collective excitations. With this assumption, the first integral in the bracket is non-zero only if $r_e(t)$ lies outside the nucleus and the second one is always very small in comparison to the first: it contains the factor $(r_e(t)/r)$, with $r_e(t)$ smaller than the nuclear radius (we exclude in this study the case of $\lambda = 0$ transitions). Keeping then only the first integral, its upper limit can be extended to infinity. This leads to

$$b_1(T_0) = \frac{4\pi e}{i\hbar} \sum_{i=1}^Z \int d^3r_0 \rho_0^{(i)}(\vec{r}_0) \sum_{\lambda\mu} \frac{S_{\lambda\mu}(T_0, \vec{r}_0)}{2\lambda+1} \langle x_1 | \hat{Q}_{\lambda\mu} | x_0 \rangle$$

where

$$Q_{\lambda\mu} = \sum_{\sigma} \int d^3r \psi_{\text{prot}}^+(\vec{r}, \sigma) e^{i\lambda} \psi_{\text{prot}}(\vec{r}, \sigma) Y_{\lambda}^{\mu*}(\vec{r})$$

is the electric multipole operator of order λ and

$$S_{\lambda\mu}(T_0, \vec{r}_0) = \int_0^{T_0} dt \Theta(r_e(t) - R_N) e^{i\omega_N t} \frac{Y_{\lambda}^{\mu}(\vec{r}_e(t))}{[r_e(t)]^{\lambda+1}}$$

Here Θ is the usual step function ($\Theta(x) = 1$ if $x > 0$ and $\Theta(x) = 0$ if $x < 0$)

and we have assumed a spherical nucleus of radius R_N .

Using (8) and (4), the transition probability between times 0 and T_0 is

$$P(T_0) = \left(\frac{4\pi e}{\hbar}\right)^2 \sum_{i,i'=1}^Z \int d^3r_0 \int d^3r'_0 \rho_0^{(i)}(\vec{r}_0) \rho_0^{(i')}(\vec{r}'_0) \\ \times \sum_{\lambda\mu} \sum_{\lambda'\mu'} \frac{S_{\lambda\mu}^*(T_0, \vec{r}_0)}{2\lambda+1} \frac{S_{\lambda'\mu'}(T_0, \vec{r}'_0)}{2\lambda'+1} \times A$$

The quantity

$$A = \frac{1}{2I_0+1} \sum_{M_0} \sum_{M_1} \langle x_1 | \hat{Q}_{\lambda\mu} | x_0 \rangle^* \langle x_1 | \hat{Q}_{\lambda'\mu'} | x_0 \rangle$$

is readily expressed with the Wigner-Eckart Theorem and the definition

$$B(E\lambda, I_0 \rightarrow I_1) = \sum_{\mu=-\lambda}^{\lambda} \sum_{M_1=-I_1}^{I_1} |\langle x_1 | \hat{Q}_{\lambda\mu} | x_0 \rangle|^2 \quad (10)$$

of $B(E\lambda; I_0 \rightarrow I_1)$ [7]. One obtains:

$$A = \delta_{\lambda\lambda'} \delta_{\mu\mu'} B(E\lambda; I_0 \rightarrow I_1) / (2\lambda+1)$$

Taking the lowest non-zero value of λ as the most probable multipolarity of the transition, the transition probability finally is:

$$P(T_0) = \left(\frac{4\pi e}{h}\right)^2 \sum_{\mu=-\lambda}^{\lambda} \int \sum_{i=1}^Z d^3r_0 \rho_0^{(i)}(\vec{r}_0) |S_{\lambda\mu}(T_0, \vec{r}_0)|^2 \frac{B(E\lambda)}{(2\lambda+1)^3} \quad (11)$$

with

$$\lambda = |I_1 - I_0| \neq 0$$

In the following we shall first base our discussion on the partial transition probability:

$$P(T_0, \vec{r}_0) = \left(\frac{4\pi e}{h}\right)^2 \sum_{\mu=-\lambda}^{\lambda} |S_{\lambda\mu}(T_0, \vec{r}_0)|^2 \frac{B(E\lambda)}{(2\lambda+1)^3} \quad (12)$$

and the one-electron transition probabilities:

$$p^{(i)}(T_0) = \int d^3r_0 \rho_0^{(i)}(\vec{r}_0) P(T_0, \vec{r}_0) \quad (13)$$

How the complete transition probability (11) can be related to (12) and (13), that is the effect of the coherence of the motion of the electrons, will be discussed in the next Section.

Finally, the transition probabilities (12) and (13), derived for one laser cycle T_0 , will be readily extended to one laser pulse $T_p = N \cdot T_0$ ($N \approx 300$). In fact, as we shall see in the next Section, the transition probabilities for one cycle are small and first order perturbation theory is still valid during one laser pulse. Replacing then T_0 by T_p in (12) and using the periodicity of the integrand of $S_{\lambda\mu}(T_0, \vec{r}_0)$, one finds that $P(T_p, \vec{r}_0)$ is equal to $N \cdot P(T_0, \vec{r}_0)$ if $\hbar\omega_N/\hbar\omega_0$ is close to an integer and vanishingly small otherwise. Consequently, during one laser pulse, only those nuclear

transitions whose energies are an integer number of times the laser photon energy can be excited by the moving electrons.

III. RESULTS.

We first study the behaviour of the probability $P(T_0, \vec{r}_0)$ of eq. (12).

This quantity depends on:

- the parameters $r_{10} = (x_0^2 + y_0^2)^{1/2}$ and z entering \vec{r}_0 (the detailed expressions developed in the Appendix show that (12) depends on x_0 and y_0 only through the combination r_{10}).
- the energy $M\omega_N$ and the multipolarity λ of the nuclear transition.
- the frequency ω_0 and the maximum electric field strength E_0 of the laser (treated as an incident classical external electro-magnetic field).

In most applications, we suppose that the laser works in the ultraviolet frequency range ($M\omega_0 = 5$ eV), and gives an electric field strength E_0 between one and five atomic units e/a_0^2 ($a_0 = .529 \cdot 10^{-8}$ cm). This corresponds to an electromagnetic intensity between $7 \cdot 10^{16}$ and $2 \cdot 10^{18}$ W/cm². These characteristics are similar to those envisaged by Boyer and Rhodes [6]. With these parameters, the amplitude of the sinusoidal motion of the electrons is greater than:

$$\gamma = \frac{eE_0}{m\omega_0^2} \sim 30 a_0 \quad (15)$$

The numerical application we have performed applies to the ^{235}U nucleus ($Z = 92$, $R = .14 \cdot 10^{13} a_0$) and the $B(E\lambda)$ in eq. (12) has been taken to be one Weisskopf unit (we assume the nucleus is spherical with radius R_N):

$$B(E\lambda) = \frac{e^2}{4\pi} \left(\frac{3}{\lambda+3}\right)^2 (R_N)^{2\lambda} \quad (16)$$

The one-electron transition probability (12) has been computed using the method described in the Appendix. The dependence of $P(T_0, \vec{r}_0)$ on r_{10} is displayed in the Figures (1a) to (1c) for some sets of the other parameters. The observed variations appear very well reproduced by the formula (A-22) and (A-25) derived in the part 2 of the Appendix. They can be rewritten here:

$$P(T_0, r_{10}, Z_0) \leq \begin{cases} P(T_0, r_{10} = R_N, Z_0) & r_{10} \leq R_N \\ P(T_0, r_{10} = R_N, Z_0) \times \left(\frac{R_N}{r_{10}}\right)^{2\lambda} & R_N \leq r_{10} \leq R_{\max} \end{cases} \quad (17)$$

where $R_{\max} \sim 5 a_0$ is much larger than the atom radius. In all the calculations we have done, the prescription of (17) is very accurately followed.

Since $P(T_0, r_{10}, Z_0)$ is maximum for $r_{10} = R_N$, we now concentrate on the behaviour of $P(T_0, r_{10} = R_N, Z_0)$ as a function of Z_0 and of the other parameters.

First, the dependence of this quantity on λ and on the laser flux ϕ is, in all the calculations, very closely reproduced by the eq. (A-28) derived in the part 2-b/ of the Appendix. Namely:

$$P(T_0, r_{10} = R_N, Z_0) \propto \frac{1}{\phi} \frac{1}{(2\lambda+1)^4 (\lambda+3)^2} \quad (18)$$

The decrease of the transition probability when ϕ increases may seem surprising. This behaviour, however, is easily understood from the relation (15) between ϕ and the amplitude γ of the electron motion: when ϕ increases and the frequency remains fixed, the electrons move farther from the nucleus

and the average Coulomb field experienced by the nucleus decreases. The dependence (18) on λ shows that the transition probability for $\lambda = 1$ is 12 times the one for $\lambda = 2$ and 67 times the one for $\lambda = 3$.

The figures (2a) to (2c) display the variation of $P(T_0, r_{\perp 0} = R_N, z_0)$ as a function of the initial position z_0 of the electron for different values of $M\omega_0$ and $M\omega_N$. One observes that the probability is quasi-periodic and becomes very small for some values of z_0 . The period of the oscillations tends to be larger as $M\omega_0$ and $M\omega_N$ decrease. This behaviour can be understood by looking at the formula (A-28) of the Appendix: the probability is proportional to $(\cos(\alpha_0 \omega_N / \omega_0))^2$ with $z_0 - \gamma \cos \alpha_0 = 0$. When $z_0 \ll \gamma$, $\alpha_0 \sim \pi/2 - z_0/\gamma$ and the period with respect to z_0 of this term approximately is

$$\pi \gamma \frac{\omega_0}{\omega_N} = \pi \frac{e}{m} \frac{E_0}{\omega_0 \omega_N}$$

We now examine the one-electron transition probability (13). In the part 3 of the Appendix, we show that an upper limit for this probability is given by (see (A-45)):

$$p^{(i)}(T_0) = p^{\max}(T_0, r_{\perp 0} = R_N) \times (D^{n\ell j} + E^{n\ell j}) \quad (19)$$

with

$$p^{\max}(T_0, r_{\perp 0} = R_N) = \text{Max}_{|z_0| \leq R_{\max}} P(T_0, r_{\perp 0} = R_N, z_0) \quad (20)$$

Here the electron i is supposed to belong to the $(n\ell j)$ shell. The multipolarity-dependent coefficients k_λ are given by (A-43): $k_1 = 3.5$, $k_2 = 1.3$ and $k_\lambda = 1.0$ for $\lambda \geq 3$. $D^{n\ell j}$ and $E^{n\ell j}$ can be found for ^{235}U in the Table I.

The values of the P^{Max} of eq. (20) are listed in the second column of the Table II for different sets of the parameters $M\omega_N$, $M\omega_0$ and λ . We have assumed $\phi = 7 \cdot 10^{16} \text{ W/cm}^2$ for the laser intensity since the probability corresponding to other values of ϕ can be obtained exactly from eq. (18). One can verify that the behaviour of (20) with λ and $M\omega_0$ follows - with an accuracy of about 8-9% - the formula (A-31) of the Appendix. Using dimensionless quantities and allowing $B(E\lambda)$ to be different from one Weisskopf unit, this formula can be rewritten here:

$$P^{\text{Max}}(T_0, r_{10} = R_N) = \frac{(M\omega_0/5\text{eV})^2}{\phi/\phi_0} \frac{B(E\lambda)}{(2\lambda+1)^4 (\lambda+3)^2} C(M\omega_N) \quad (21)$$

where $\phi_0 = 7 \cdot 10^{16} \text{ W/cm}^2$ and $B(E\lambda)$ is expressed in Weisskopf units. Let us recall that this expression can be used only if the amplitude $\gamma = e E_0 / m\omega_0^2$ is much larger than the atom radius. Using Table II it appears that $C(M\omega_N)$ is a very slowly changing function of $M\omega_N$. It takes values between 40 and 60 for $20 \text{ eV} < M\omega_N < 500 \text{ keV}$. This result may appear surprising in view of the form (9) of $S(T_0, \vec{r}_0)$: one expects that the exponential factor averages the integral to zero when ω_N is large. In fact, the expressions developed in the Appendix reveal that only the values of t belonging to a very small interval Δt give a significant contribution to the integral. The discussion leading to the formula (A-29) shows that $\Delta t \sim R_N / (\gamma \omega_0) \approx \frac{R_N}{2\pi\gamma} T_0 \approx 10^{-6} T_0$. It follows that, unless $M\omega_N$ larger than at least 1 MeV, the exponential in (9) does not oscillate in the interval Δt and consequently the integral is not expected to go to zero. From a physical point of view, this result means that the electrons are actually effective in exciting the nucleus only during the very short time they spend in the vicinity of the nucleus, that is, when the Coulomb field experienced by the nucleus is maximum. As a matter of fact,

Δt is approximately the time required by a electron moving according to (1) with $r_{10} = 0$ to pass through the nucleus. However, this independence of the laser frequency from the nuclear transition is misleading. The number of cycles in a laser pulse, assumed to be 300 cycles in our case, restricts the nuclear transition to an integer multiple of the laser frequency. Practical considerations will restrict this multiple to an integer low enough to manage this energy matching.

The values listed in Table I show that the one-electron probability (19) is maximum for electrons belonging to the 1s and 2s shells, whatever the value of λ . The probability induced by one electron of the 3s1/2, 2p1/2 and 4s1/2 shells are 4%, 2% and 1% respectively the one induced by a 1s electron. Electrons on the other shells contribute only less than 1%. This remark has important consequences concerning the effect of possible coherence of the motion of the electron cloud, that is the relation between the total transition probability (11) and the one-electron transition probabilities (13). In fact, the summation over i in (11) can be restricted to the 4 electrons belonging to the 1s and 2s shells. Consequently:

$$P(T_0) \approx 4 \sum_i P^{(i)}(T_0) \quad (22)$$

with $P(T_0)$ given by (13) and (19). The effect of the coherence of the electron motion is therefore to multiply the incoherent transition probability by a factor of 4. This is much less than the Z factor that would have appeared by directly trying to majorate the square of the sum over i in (11).

Finally, the third column of Table II displays what we obtain as an upper limit for the incoherent transition probability induced by all the atomic electrons. It has been obtained by summing (19) over all the atomic shells.

According to (22), the total coherent transition probability is about 4 times larger.

At this point, we would like to stress that the inner shells - whose contribution to the total probability is maximum - are occupied by the most tightly bound electrons. As shown in Table I, the binding energies of the 1s, 2s and 2p electrons are larger than 15 keV. Since the kinetic energy of a free electron is, with the laser parameters we have adopted, at most 4 keV, it is very unlikely that the electrons belonging to these shells can be set into motion by the laser. In addition, the electric field experienced by the innermost electrons certainly is considerably screened by the electrons belonging to the other shells. Table I also shows that the electrons belonging to the 3s, 3p and 3d shells have binding energies in the range 3-5 keV. The influence of the laser on these electrons may therefore be questionable. However, as we want to keep the possibility of dealing with high laser fluxes and, furthermore, are interested in deriving upper limits to the nuclear transition probabilities, we shall assume that the electrons of these latter shells do contribute to the nuclear excitation. Due to this remark, one should therefore be aware that the probabilities obtained when including all the Uranium electrons are very strongly overestimated. For this reason, we have listed in Table II the transition probabilities computed: a/ from the two 3s electrons which are the most bound ones that may contribute (fourth column), b/ when excluding the 1s and 2s electrons (fifth column) and c/ when excluding the 1s, 2s and 2p electrons (sixth column). The latter values certainly are the closest to reality and will be used in the following applications. Inclusion of coherence effects would, as before, result in a factor of 4 since, in this case, the 3s and 4s shells give the major part of the transition probability.

IV. APPLICATION TO THE POPULATION OF THE 75 eV ISOMER OF ^{235}U .

Given the nuclear transition probabilities per laser cycle found in the preceding Section, it is interesting to estimate what would be the number of excited nuclei actually produced in a laser-induced excitation experiment. We choose, as before, to excite the 26 minutes, 75 eV isomer of ^{235}U , and assume this can be done by means of the following experimental set-up. A sample of ^{235}U hexafluoride gas is enclosed in a small container sitting in vacuum. The laser beam passes through the container by means of windows and is focused in the center of the container. For reasons related to the technology of highly transparent windows, the gas pressure inside the container is assumed to be only 1 Torr (1/760 atmosphere) at normal temperature [11]. In this situation, all the nuclei contained in the laser focus volume can be supposed to experience the full laser flux and energy [12]. The laser characteristics we choose are those considered previously: photon energy $h\nu_0 = 5$ eV, flux $\phi = 7 \cdot 10^{16}$ to $2 \cdot 10^{18}$ W/cm^2 , pulse duration = 300 laser cycles ($\sim 2 \cdot 10^{-13}$ s.), pulse repetition rate: one per second, focus volume $(10 \text{ } \mu\text{m})^3$. With the latter figure one finds that the number of ^{235}U nuclei involved in the excitation process is $\sim 3 \cdot 10^7$. We assume the experiment can be carried out during the whole isomer lifetime without change in the number of U nuclei contained in the focus volume.

Table III displays upper limits for the number of isomers that could be produced in such an experiment. The contributions of different electrons shells are displayed. In each case, we have listed the upper limit of the nuclear transition probability per laser cycle (taken from the line $h\nu_N = 75$ eV, $h\nu_0 = 5$ eV, $\lambda = 3$ of Table II) and the isomer yields corresponding to different exposure times. We first give the number of isomers produced by the

motion of the two electrons of the $3s_{1/2}$ shell since, as was discussed previously, they are the deepest electrons that are likely to be set into motion by the laser (their binding energy is comparable to the kinetic energy of a free electron in the electric field of a laser of flux 10^{18} W/cm^2). As expected, their contribution is fairly large: it represents 60% that of the 80 less bound electrons. The last two lines include the contribution of the 2p, 2s and 1s shells. Although these shells will not participate in the nuclear excitation, we have displayed the corresponding isomer yields to show what would be the results if they were incorrectly taken into account. The maximum number of isomers that could be produced in the envisaged experiment during the level lifetime does not exceed 50-60,000. One must recall (end of Section II) that the nuclear transition must be an integer multiple of the laser frequency. Whether or not this yield would support a viable experimental measurement, we leave to the expertise of our more practical colleagues.

V. APPLICATION TO THE TRANSFER FROM THE STORAGE LEVEL TO THE LASING STATE.

As a second application, we now study if the excitation mechanism analyzed in this work can be used to induce the lasing phase of a gamma-ray laser, that is, to cause the transfer from the storage level to a short-lived state lying higher in energy. Our discussion will be based on the nuclear transition probability per laser pulse $P(T_p)$ deduced from (19). Taking as before the pulse duration to be 300 cycles, we have:

$$P(T_p) \approx 300 P^{\text{Max}}(T_0, r_{10} = R_N) \sum_{n, l, j} g^{n, l, j} (D^{n, l, j} + k_\lambda E^{n, l, j}) \quad (23)$$

where the summation over (nlj) extends to the electron shells participating to the nuclear excitation. We first assume the laser photon energy is $\hbar\omega_0 = 5$ eV, the laser flux is $\phi = \phi_0 = 7 \cdot 10^{16}$ W/cm² and all electrons except those of the 1s, 2s and 2p shells participate to the excitation. The quantity $P^{\text{Max}}(T_0, r_{10} = R_N)$ is then very well reproduced by eq. (21). The transfer probabilities obtained from (23) in this case are listed in Table IV for $B(E\lambda) = 1$ Weisskopf unit and different values of the multipolarity λ of the nuclear transition. Let us recall that the results are almost independent of the energy of the transition between 20 eV and 500 keV although the experimental problem of matching the nuclear transition energy to an integral multiple of the laser frequency will limit the magnitude of this ratio (we have taken $C(\hbar\omega_N) = 50$ in (21)). It appears that in order to obtain a transfer probability per pulse larger than 10^{-4} - a value that seems at least desirable - with the above laser characteristics, one has to choose a nuclear transition of multipolarity $\lambda = 1$ and preferentially of collective nature ($B(E\lambda) \geq 1$).

It must be noted that acting on the parameters $\hbar\omega_0$ and ϕ of the laser would not help much in improving the transfer probabilities. At first sight, it seems that increasing the ratio $(\hbar\omega_0)/\phi$ contained in $P^{\text{Max}}(T_0, r_{10} = R)$ would be useful. However, since the average kinetic energy acquired by one electron from the laser is inversely proportional to this ratio, less electron shells are expected to participate to the nuclear excitation and the sum in (23) tends to decrease. For instance, if the above ratio is multiplied by 10, only the 5s and less bound shells should, in the best case, be included and the probability $P(T_p)$ increases by a factor of at most 5. Higher values of the ratio would result in no electron motion at all. We would stress, however, that the case of low flux and high $\hbar\omega_0$ is somewhat beyond the limits of the

model used in this work which neglects the influence of the central Coulomb potential on the motion of the electrons.

VI. CONCLUSIONS.

A realistic but computationally simple model has been employed to examine nuclear transitions induced by laser-electron coupling. Applications to both test the model and to design criteria for a gamma-ray laser have been made. Nearly independent of laser characteristics we find the percentage of nuclear transitions of multipolarity λ to be

$$\approx 10^{-(3+\lambda)} \quad , \quad \lambda = 1, 2, 3$$

for 1 Weisskopf unit transition matrix element.

Most electromagnetic transitions between nuclear states have strengths several orders of magnitude less than 1 Weisskopf unit. In particular, one can expect the transition between a spin isomeric state and a proximate lasing state to be severely inhibited. Therefore, these results emphasize the importance of finding isomeric states of a collective nature.¹³ They also indicate the value of a quantum mechanical calculation of this motion such as that of ref. (4) which would include self shielding and a more precise treatment of electron currents near the nucleus. Lastly, we must also conclude that an alternative regime for the switching mechanism would be highly desirable.

APPENDIX.

This Appendix is divided into three parts. In the first, we develop expressions that permit to evaluate numerically the nuclear transition probability (12). Approximate formula displaying the behaviour of this transition probability are derived in the second part. The third one presents the method used for averaging over the initial positions of electrons. When numerical examples are given, lengths are expressed in units of $a_0 = .529 \cdot 10^{-8}$ cm.

The transition probability (12) reads:

$$P(T_0, \vec{r}_0) = \left(\frac{4\pi e}{h}\right)^2 \sum_{\mu=-\lambda}^{\lambda} |S_{\lambda\mu}(T_0, \vec{r}_0)|^2 \frac{B(E\lambda)}{(2\lambda+1)^3} \quad (A-1)$$

with

$$S_{\lambda\mu}(T_0, \vec{r}_0) = \int_0^{t_0} e^{i\omega_N t} \Theta(r(t) - R_N) \frac{Y_{\lambda\mu}(\vec{r}(t))}{[r(t)]^{\lambda+1}} dt \quad (A-2)$$

and

$$r(t) = (r_{10}^2 + z(t)^2)^{1/2} \quad z(t) = z_0 - \gamma \sin \omega_0 t \quad (A-3)$$

The two angles defining the direction of $\vec{r}(t)$ are symbolized by $\hat{r}(t)$.

1- Expression of $S_{\lambda\mu}(T_0, \vec{r}_0)$.

We first re-express $S_{\lambda\mu}$ with the formula:

$$r^\lambda Y_{\lambda\mu}(\hat{r}) = C_{\lambda\mu} (x+iy)^\mu (r_\perp)^{\lambda-\mu} P_{\lambda\mu}(z/r_\perp) \quad (A-4)$$

with $r_\perp = (r^2 - z^2)^{1/2}$. The constants $C_{\lambda\mu}$ and the polynomials $P_{\lambda\mu}$ are given in Table A-1 for $\lambda = 1, 2$ and 3 . Then, we make the change of variables $t \rightarrow \alpha = \omega_0 t$ and introduce the variable $v = z/r_{10}$ (we assume $r_{10} \neq 0$). This gives:

$$|S_{\lambda\mu}(T_0, \vec{r}_0)| = \frac{C_{\lambda\mu}}{\omega_0} \frac{|I_{\lambda\mu}|}{(r_{10})^{\lambda+1}} \quad (A-5)$$

with

$$I_{\lambda\mu} = \int_0^{2\pi} d\alpha \, e^{i\frac{\omega_N}{\omega_0} \alpha} \Theta(r(\alpha) - R_N) f_{\lambda\mu}(v(\alpha)) \quad (A-6)$$

$$f_{\lambda\mu}(v) = \frac{P_{\lambda\mu}(v)}{(1+v^2)^{\lambda+1/2}} \quad (A-7)$$

$$r(\alpha) = (r_{10}^2 + z^2(\alpha))^{1/2} \quad v(\alpha) = \frac{z(\alpha)}{r_{10}} = \frac{z - \gamma \sin \alpha}{r_{10}} \quad (A-8)$$

The functions $f_{\lambda\mu}$ appearing in (A-6) are regular and take very small values except for $|v| \leq 5$. However, the integration in (A-6) cannot be easily done, especially when r_{10} is small. In fact, for $r_{10} = R_N = .14 \cdot 10^{-3}$, a typical integration step would be $\Delta\alpha = \Delta v \cdot r_{10} / \gamma \sim 10^{-7}$ with $\Delta v = 10^{-2}$ and $\gamma = 20 a_0$ (a value of λ shown in Section III to correspond to presently available intense lasers). We therefore transform the integral in the following way. First, we change the integration interval from $[0, 2\pi]$ to $[0, \pi/2]$ by splitting it into four equal intervals and making appropriate changes of variable. This gives

$$I_{\lambda\mu} = 2e^{i\pi\frac{\omega_N}{\omega_0}} (J_{\lambda\mu}^- + e^{i\pi\frac{\omega_N}{\omega_0}} J_{\lambda\mu}^+) \quad (A-9)$$

with

$$J_{\lambda\mu}^\pm = \int_0^{\pi/2} d\alpha \, \Theta(r^\pm(\alpha) - R_N) \cos \frac{\omega_N}{\omega_0} \alpha f_{\lambda\mu}(u^\pm(\alpha)) \quad (A-10)$$

and

$$u^\pm(\alpha) = (z_0 \pm \gamma \cos \alpha) / r_{10} \quad r^\pm(\alpha) = r_{10} (1 + u^\pm(\alpha)^2)^{1/2} \quad (A-11)$$

The $[0, \pi/2]$ interval is then further split into intervals $[\alpha_a, \alpha_b]$ such that $r^\pm(\alpha) > R_N$ and $|u^\pm(\alpha)| < u_M \approx 5$. The integrals (A-10) therefore become sums of integrals of the form

$$J_{\lambda\mu}^\pm = \sum_k \int_{\alpha_a^k}^{\alpha_b^k} d\alpha \cos \frac{\omega_N}{\omega_0} \alpha f_{\lambda\mu}(u^\pm(\alpha)) \quad (\text{A-12})$$

In order to carry out the integration numerically, we choose a step $\Delta\alpha$ such that $\Delta\alpha \omega_N/\omega_0 \ll 1$. Eq. (A-12) can thus be approximately replaced by:

$$J_{\lambda\mu}^\pm = \sum_k \sum_{j=1}^{N_k} \cos \frac{\omega_N}{\omega_0} \alpha_{j-1/2} \int_{\alpha_{j-1}}^{\alpha_j} d\alpha f_{\lambda\mu}(u^\pm(\alpha)) \quad (\text{A-13})$$

with

$$\alpha_0 = \alpha_a^k \quad \alpha_j = \alpha_0 + j\Delta\alpha \quad \alpha_{N_k} = \alpha_b^k$$

We now make the change of variables $\alpha \rightarrow u = u^\pm(\alpha)$. Since $\omega_N/\omega_0 > 1$ in general, the Jacobian

$$du/d\alpha \equiv \pm \frac{Y}{r_{10}} \sin \alpha \quad (\text{A-14})$$

is approximately constant in each interval $[\alpha_{j-1}, \alpha_j]$ with the value

$$\pm \frac{Y}{r_{10}} \sin \alpha_{j-1/2} \approx \frac{u^\pm(\alpha_j) - u^\pm(\alpha_{j-1})}{\Delta\alpha} \quad (\text{A-15})$$

This finally leads to

$$J_{\lambda\mu}^\pm = \sum_k \Delta\alpha \sum_{j=1}^{N_k} \cos \frac{\omega_N}{\omega_0} \alpha_{j-1/2} \frac{F_{\lambda\mu}(u^\pm(\alpha_j)) - F_{\lambda\mu}(u^\pm(\alpha_{j-1}))}{u^\pm(\alpha_j) - u^\pm(\alpha_{j-1})} \quad (\text{A-16})$$

with

$$F_{\lambda\mu}(u) = \int du f_{\lambda\mu}(u) \quad (A-17)$$

The $F_{\lambda\mu}(u)$ can be expressed analytically. They are given in Table A-I for $\lambda = 1, 2$ and 3 . Expression (A-16) is therefore very easy to evaluate numerically. Besides, the number of steps N_α required is quite reasonable: it remains lower than 5000 for $\hbar\omega_N < 500$ keV.

The explicit forms of the $f_{\lambda\mu}$, (A-11) and (A-12) show that changing z_0 into $-z_0$ transforms $f_{\lambda\mu}(u^\pm(\alpha))$ into $(-)^{\lambda+\mu} f_{\lambda\mu}(u^\pm(\alpha))$ and, consequently, $J_{\lambda\mu}^\pm$ into $(-)^{\lambda+\mu} J_{\lambda\mu}^\pm$. Therefore, $|I_{\lambda\mu}|$ is unchanged and

$$P(T_0, r_{\perp 0}, -z_0) = P(T_0, r_{\perp 0}, z_0) \quad (A-18)$$

Similarly, changing μ into $-\mu$ transforms $(x + iy)^\mu$ of (A-4) into $(-x + iy)^\mu$. Consequently, $|S_{\lambda\mu}(T_0)|$ is unchanged and only the positive or zero values of μ have to be considered.

2- Approximate expressions for the transition probability.

a/ We first examine the behaviour of $|I_{\lambda\mu}|$ and $P(T_0, r_{\perp 0}, z_0)$ with $r_{\perp 0}$. The amplitude γ of the electron motion is assumed to be much larger than the atom radius, a condition fulfilled in the applications we consider (the laser parameters $\hbar\omega_0 = 5$ eV and $\phi = 7 \cdot 10^{16}$ W/cm² lead to $\gamma > 30 a_0$). In this case the values of $r_{\perp 0}$ and z_0 of interest are much smaller than γ . Starting from (A-6), the variation $\Delta\alpha$ of α in the range $|v| < 5$ where $f_{\lambda\mu}(v(\alpha))$ is non-negligible is very small. In fact, from (A-8), $\Delta\alpha$ is given by

$$\mp \frac{\gamma}{r_{\perp 0}} \cos \alpha_0^\pm \Delta\alpha \approx 10$$

with

$$z_0 - \gamma \sin \alpha_0^+ = 0$$

that is:

$$\alpha_0^+ = z_0/\gamma, \quad \alpha_0^- = \pi - z_0/\gamma, \quad |\Delta\alpha| \approx 10 \frac{r_{\perp 0}}{\gamma}$$

Assuming ω_N/ω_0 is not too large, namely:

$$\frac{\omega_N}{\omega_0} \ll \gamma/r_{\perp 0} \quad (\text{A-19})$$

the exponential can be taken out of the integral (A-6). Hence:

$$I_{\lambda u} \approx e^{i \frac{\omega_N}{\omega_0} \alpha_0^+} \int_{\alpha_0^+ - \frac{\Delta\alpha}{2}}^{\alpha_0^+ + \frac{\Delta\alpha}{2}} d\alpha \Theta(r(\alpha) - R_N) f_{\lambda u}(v(\alpha)) \quad (\text{A-20})$$

$$+ e^{i \frac{\omega_N}{\omega_0} \alpha_0^-} \int_{\alpha_0^- - \frac{\Delta\alpha}{2}}^{\alpha_0^- + \frac{\Delta\alpha}{2}} d\alpha \Theta(r(\alpha) - R_N) f_{\lambda u}(v(\alpha))$$

In the case $r_{\perp 0} > R_N$ (but still $r_{\perp 0} \ll \gamma$), the Θ -function is unity and both integrals can be approximated by:

$$\frac{d\alpha}{dv}(\alpha_0^\pm) \int_{-a}^{+a} dv f_{\lambda u}(v)$$

Since

$$\left| \frac{dv}{d\alpha}(\alpha_0^\pm) \right| = \frac{\gamma}{r_{\perp 0}} |\cos \alpha_0^\pm| \approx \frac{\gamma}{r_{\perp 0}}$$

one obtains

$$I_{\lambda\mu} \approx e^{i \frac{\omega_N}{\omega_0} \frac{\pi}{2}} 2 \cos \frac{\omega_N}{\omega_0} (\pi/2 - z_0/\gamma) \cdot \frac{r_{10}}{\gamma} \int_{-\infty}^{+\infty} dv f_{\lambda\mu}(v) \quad (A-21)$$

Consequently, $|I_{\lambda\mu}|$ is proportional to r_{10} :

$$|I_{\lambda\mu}(r_{10})| \sim I_{\lambda\mu}(r_{10} = R_N) \times \frac{r_{10}}{R_N}$$

and therefore:

$$P(T_0, r_{10}, z_0) \sim P(T_0, r_{10} = R_N, z_0) \times \left(\frac{R_N}{r_{10}}\right)^{2\lambda} r_{10} \geq R_N \quad (A-22)$$

In the case $r_{10} < R_N$, the values of v such that $v^2 < \left(\frac{R_N}{r_{10}}\right)^2 - 1$ have to be excluded from the integration range in (A-21). When r_{10} is smaller than $R_N / 5$, the values of v that remain are larger than 5 and the $f_{\lambda\mu}(v)$ can be replaced by their asymptotic forms. It is then easy to show that the integral is close to zero if $\lambda + \mu$ is odd and behaves as $(r_{10})^{\lambda+\mu}$ otherwise. When r_{10} is larger than $R_N/5$ and approaches R_N , the interval of excluded v -values shrinks and tends to zero. The integral of (A-21) then behaves - when non-zero - as r_{10}^β with $1 \leq \beta < \lambda + \mu + 1$. From this we deduce:

$$|I_{\lambda\mu}(r_{10})| \leq |I_{\lambda\mu}(r_{10} = R_N)| \left(\frac{r_{10}}{R_N}\right)^{\lambda+\mu+1} \quad (A-24)$$

and, consequently:

$$P(T_0, r_{10}, z_0) \leq P(T_0, r_{10} = R_N, z_0) r_{10} \leq R_N \quad (A-25)$$

The dependence of $P(T_0)$ on r_{10} displayed in (A-22) and (A-25) is very accurately reproduced by the numerical calculations.

b/ We now concentrate on the behaviour of $P(T_0, r_{\perp 0} = R_N, z_0)$ as a function of the other parameters. From the discussion developed in a/, I is given by (A-21) with $r_{\perp 0} = R_N$. Inserting these expressions into (A-5) and (A-1), one gets:

$$P(T_0, r_{\perp 0} = R_N, z_0) = \frac{A_\lambda^2}{R_N^{2\lambda} (\gamma \omega_0)^2} \cos^2 \left(\frac{\omega_N}{\omega_0} \alpha_0 \right) \cdot \frac{B(E\lambda)}{(2\lambda + 1)^3} \quad (A-26)$$

with

$$A_\lambda = \frac{8\pi e}{\hbar} \sum_{\mu=-\lambda}^{\lambda} 2 C_{\lambda\mu} \int_{-\infty}^{\infty} dV f_{\lambda\mu}(V) = \frac{32\pi e}{\hbar} C_{\lambda\lambda} F_{\lambda\lambda}(+\infty) \quad (A-27)$$

and $\alpha_0 = \frac{\pi}{2} - \frac{z_0}{\gamma}$. The quantity A_λ is approximately proportional to $(2\lambda+1)^{-1/2}$, γ is $e E_0 / m \omega_0^2$ and $B(E\lambda)$ (assuming one Weisskopf unit) is given by (16). Thus we obtain:

$$P(T_0, r_{\perp 0} = R_N, z_0) = K \left(\frac{m \omega_0}{e E_0} \right)^2 \frac{\cos^2 \left(\frac{\omega_N}{\omega_0} \alpha_0 \right)}{(2\lambda + 1)^4 (\lambda + 3)^2} \quad (A-28)$$

where K is a proportionality constant.

We note first that (A-26) is accurate as long as (A-19) is verified, that is

$$\frac{\omega_N}{\omega_0} \ll \frac{\gamma}{R_N} \quad (A-29)$$

If this condition is not fulfilled, in particular if $m \omega_N$ is much larger than $\hbar \omega_0$, $P(T_0, r_{\perp 0} = R_N, z_0)$ is expected to be lower than (A-28)

The dependence of $P(T_0, r_{\perp 0} = R_N, z_0)$ on E_0 and λ is very simple: The probability is proportional to $(E_0)^{-2}$, i.e., to ϕ^{-1} , where ϕ is the laser

intensity, and P is larger for lower multiplicities. This behaviour as a function of E_0 and λ is very well reproduced by the numerical calculations.

The dependency of (A-28) on $M\omega_0$ is more complicated since ω_0 enters in particular in the definition of α_0 via the amplitude γ . Some information can be drawn however from this expression if one considers the maximum value:

$$P^{\text{Max}}(T_0, r_{\perp} = R_N) = \max_{|z_0| \leq R_{\text{Max}} \sim 5a_0} P(T_0, r_{\perp 0} = R_N, z_0) \quad (\text{A-30})$$

obtained when taking into account the dependence on z_0 . This quantity will be shown to play an important role when averaging the transition probability over the initial locations of the electrons (see part 3/, eq. (A-32)). The expression (A-28) is periodic with respects to z_0 - which is confirmed by the numerical calculations (see the figures 2a to 2c) -, and consequently, the maximum (A-30) will be obtained when $\frac{\omega_N}{\omega_0} \alpha_0$ is an integer multiple of π . From this we deduce that (A-30) is approximately proportional to the square of the laser frequency. Using (A-28), we then obtain:

$$P^{\text{Max}}(T_0, r_{\perp 0} = R_N) = \frac{(M\omega_0)^2}{\Phi} \frac{K(M\omega_N)}{(2\lambda+1)^4 (\lambda+3)^2} \quad (\text{A-31})$$

where $K(M\omega_0)$ is function of the nuclear transition energy only.

3- Average over the initial position of the electrons.

Equation (13) of section II can be rewritten:

$$P^{(i)}(T_0) = 2\pi \int_0^{\infty} r_{\perp 0} dr_{\perp 0} \int_{-\infty}^{+\infty} dz_0 \rho_0^{(i)}(r_{\perp 0}, z_0) P(T_0, r_{\perp 0}, z_0)$$

where $\rho_0^{(i)}(r_{\perp 0}, z_0)$ is the probability of finding - before laser excitation - the i -th electron in the annular volume element $2\pi r_{\perp 0} dr_{\perp 0} dz_0$. We assume the

electron distribution symmetric with respect to the x-y plane, that is $\rho_0^{(i)}(r_{10}, z_0) = \rho_0^{(i)}(r_{10}, -z_0)$ and use the majorations (A-22)-(A-25) of the transition probability. This leads to

$$p^{(i)}(T_0) \leq 4\pi \int_0^\infty dz P(T_0, r_{10} = R_N, z) \quad (A-32)$$

$$\times \left[\int_0^{R_N} r_\perp dr_\perp \rho_0^{(i)}(r_\perp, z) + \int_{-\infty}^{+\infty} \left(\frac{R_N}{r_\perp}\right)^{2\lambda} \rho_0^{(i)}(r_\perp, z) r_\perp dr_\perp \right]$$

The numerical calculations show that $P(T_0, r_{10} = R_N, z)$ is a smooth function of z . We therefore introduce the upper limit:

$$p^{\text{Max}}(T_0, r_{10} = R_N) = \max_{t \leq R_{\text{Max}}} P(T_0, r_{10} = R_N, z) \quad (A-33)$$

where R_{Max} is a radius such that the density $\rho_0^{(i)}$ in Uranium is negligible (for instance, $R_{\text{Max}} = 10 a_0$). Then, we introduce polar coordinate (r, θ) in place of the cylindrical ones. Developing the condition $r_\perp = r \sin \theta \begin{matrix} > \\ < \end{matrix} R_N$ leads to

$$p^{(i)}(T_0) \leq p^{\text{Max}}(T_0, r_{10} = R_N) \times (D^{(i)}(R_N) + G^{(i)}(R_N)) \quad (A-34)$$

with

$$D^{(i)}(R_N) = 4\pi \int_0^{R_N} r^2 dr \int_0^{\pi/2} d\theta \sin \theta \rho_0^{(i)}(r, \theta) \quad (A-35)$$

$$G^{(i)}(R_N) = 4\pi \int_{R_N}^{R_{\text{Max}}} r^2 dr A^{(i)}(r) \quad (A-36)$$

$$A^{(i)}(r) = \int_0^{\theta_N(r)} \sin \theta d\theta \rho_0^{(i)}(r, \theta) + \int_{\theta_N(r)}^{\pi/2} d\theta \sin \theta \left(\frac{R_N}{r \sin \theta}\right)^{2\lambda} \rho_0^{(i)}(r, \theta) \quad (A-37)$$

The angle $\theta_N(r)$ is given by

$$\sin\theta_N(r) = \frac{R_N}{r}, \quad 0 \leq \theta_N(r) \leq \pi/2 \quad (\text{A-38})$$

and the quantity $D^{(i)}(R_N)$ is the probability of finding the electron (i) inside the nucleus.

We now determine an upper limit for $G^{(i)}(R_N)$. To this aim, we first average over the g_{nlj} electrons (i) belonging to the same shell (nlj). The average of $\rho_0^{(i)}(r, \theta)$ with respect to (i) is independent of θ if the shell is closed:

$$\frac{1}{2j+1} \sum_{m=-j}^j \rho_0^{(nljm)}(r, \theta) = \rho_0^{nlj}(r) \quad (\text{A-39})$$

If the shell is open, the average $\frac{1}{g_{nlj}} \sum_m \rho_0^{nljm}(r, \theta)$ is lower than $(2l+1) \times \rho_0^{(i)}(r)$. Consequently, for a electron (i) belonging to the (nlj)-shell:

$$G^{(i)}(R_N) \leq 4\pi K_l \int_{R_N}^{R_{\text{Max}}} r^2 dr \rho_0^{(nlj)}(r) I_\lambda(r) \quad (\text{A-40})$$

with

$$\begin{aligned} K_l &= 1 && \text{if the (nlj)-shell is closed} \\ K_l &= 2l+1 && \text{if the (nlj)-shell is open} \end{aligned} \quad (\text{A-41})$$

and

$$I_\lambda(r) = 1 - \cos\theta_N(r) + \int_{\theta_N(r)}^{\pi/2} \sin\theta d\theta \left(\frac{\sin\theta_N(r)}{\sin\theta} \right)^{2\lambda} \quad (\text{A-42})$$

The functions (A-42) can be expressed analytically. They decrease from 1 to 0 when r goes from R_N to infinity. The explicit forms of these functions show that

$$I_{\lambda}(r) < k_{\lambda} \left(\frac{R_N}{r}\right)^2 \quad R_N \leq r \leq R_{\text{Max}} \sim 10a_0$$

with

$$k_1 = 3.5, \quad k_2 = 1.3, \quad k_{\lambda} = 1. \quad \text{for } \lambda \geq 3 \quad (\text{A-43})$$

We then get:

$$G^{(i)}(R_N) \leq k_2 k_{\lambda} (R_N)^2 \int_{R_N}^{R_{\text{Max}}} 4\pi dr \rho_0^{(nlj)}(r) \quad (\text{A-44})$$

The integral is lower than the expectation value $\langle r^{-2} \rangle^{(nlj)}$ of r^{-2} in the (nlj) shell. Inserting (A-44) into (A-34) finally gives the transition probability for an electron i belonging to the (nlj) shell:

$$P^{(i)}(T_0) \leq P^{\text{Max}}(T_0, r_{\perp 0} = R_N) \times [D^{(nlj)}(R_N) + k_{\lambda} E^{(nlj)}] \quad (\text{A-45})$$

with

$$E^{(nlj)} = k_2 (R_N)^2 \langle r^{-2} \rangle^{(nlj)}$$

The quantities $D^{(nlj)}$ and $\langle r^{-2} \rangle^{(nlj)}$ can be found in the literature. They are given together with $E^{(nlj)}$ in Table I for the Uranium atom.

REFERENCES

- [1] G. C. BALDWIN and J. C. SOLEM, Rev. Mod. Phys., Vol. 53, Part I (1981) 687.
- [2] K. BOYER and C. K. RHODES, Phys. Rev. Lett., Vol. 54, (1985) 1490.
A. SZÖKE and C. K. RHODES, Phys. Rev. Lett., Vol 56, (1986), 720.
- [3] P. KALMAN and J. BERGOU, Phys. Rev. C34, No 3, (1986) 1024. B. ARAD, S. ELIEZER and Y. PAISS, Phys. Lett. 74A, No. 6, (1979) 395. V. A. PLUYKO, Sov. J. Nucl. Phys. 44 (2) (1986) 231.
- [4] K. C. KULANDER, to be published in Physical Review A.
- [5] J. C. SOLEM and L. C. BIEDENHARM, LASL preprint LA-UR-86-3826.
- [6] A. P. SCHWARZENBACH, T. S. LUK, I. A. McINTYRE, U. JOHANN, A. McPHERSON, K. BOYER and C.K. RHODES, Opt. Lett., 11, (1986) 499.
- [7] A. BOHR and B. R. MOTTELSON, Nuclear Structure, Vol. 1, (Benjamin, 1969) p. 382.
- [8] K.-N. HUANG, M. AOYAGI, M. H. CHEN, B. CRASEMANN and H. MARK, Atomic Data and Nuclear Data Tables, 18 (1976) 243.
- [9] I. M. BAND and M. B. TRZHASKOVSKAYA, Atomic data and Nuclear Data Tables, 35 (1986) 1.
- [10] J. P. DESCLAUX, Atomic Data and Nuclear Data Tables, 12, No. 4 (1973) 312.
- [11] Possibly an upper limit (A. Szoke, private communication).
- [12] R. DEI-CAS, Private Communication.
- [13] M. S. WEISS, "Shape Isomers as Candidates for a Gamma Ray Laser," in preparation.

ACKNOWLEDGMENTS

The authors would like to thank D. Iracane and R. Dei-Cas for many discussions and helpful comments. Two of us (J.-F. B. and D. G.) wish to acknowledge the warm hospitality received in the Nuclear Theory Group at LLNL, where most of this work has been done. Lastly, one of us (MSW) would like to acknowledge helpful discussions with A. Szöke and C. Rhodes.

FIGURE CAPTIONS

FIGS. (1a) to (1c).

The partial transition probability $P(T_0, r_{10}, z_0)$ - Eq. (12) of the text - as a function of r_{10} for $z_0 = 2 a_0$ ($a_0 = .529 \cdot 10^{-8} \text{ cm}$) and two values of the laser flux ϕ . $\hbar\omega_0$ is the laser photon energy and $\hbar\omega_N$ the energy of the nuclear transition. The three figures correspond to the three transition multipolarities $\lambda = 1, 2$ and 3 . The scales on both axes are logarithmic, showing the linear dependence of $\text{Log}(P)$ on $\text{Log}(r_{10})$.

FIGS. (2a) to (2c).

The partial transition probability $P(T_0, r_{10} = R_N, z_0)$ as a function of z_0 for $r_{10} = R_N$, the nuclear radius. The laser flux is fixed to one atomic unit $\phi = 7 \cdot 10^{16} \text{ W/cm}^2$. λ is the multipolarity of the nuclear transition. Different values of $\hbar\omega_0$ (laser photon energy) and $\hbar\omega_N$ (nuclear transition energy) have been chosen for the three figures, showing how evolves the periodic behaviour of P when these parameters change.

TABLE CAPTIONS

- Table I. Parameters associated to the electron shells ($n\ell j$) of the ^{235}U atom. $g^{n\ell j}$ is the level degeneracy, K_ℓ an angular average parameter defined in (A-41), $\epsilon^{n\ell j}$ the single particle binding energy, $D^{n\ell j}(R_N)$ the probability of one electron of the shell to be inside the nucleus, (--- means less than 10^{-10}), $\langle r^{-2} \rangle^{n\ell j}$ the average value of r^{-2} for one electron of the shell and $E^{n\ell j} = K_\ell R_N^2 \langle r^{-2} \rangle^{n\ell j}$. R_N is the nuclear radius ($.14 \cdot 10^{-3} a_0$ for ^{235}U with $a_0 = .529 \cdot 10^{-8}$ cm).
- Table II. Values of $P^{\text{Max}}(T_0, r_{10} = R_N)$ - Eq. (20) of the text - and of the total nuclear transition probability per laser cycle when taking into account different atomic shells or groups of shells in ^{235}U . $M\omega_N$ and λ are the energy and the multipolarity of the nuclear transition respectively and $M\omega_0$ is the laser photon energy. The laser flux is assumed to be $\phi = 7 \cdot 10^{16} \text{ W/cm}^2$.
- Table III. Maximum population yields of the 75 eV, 26 mn isomeric level of ^{235}U by means of the laser+electron mechanism described in the text. The characteristics of the laser beam are the following: photon energy $M\omega_0 = 5 \text{ eV}$, flux $\phi = 7 \cdot 10^{16} \text{ W/cm}^2$, focus volume: $(10 \text{ } \mu\text{m})^3$, pulse duration 300 laser cycles ($\sim 2 \cdot 10^{-13} \text{ s}$), pulse repetition rate: one per second. The exposed material is assumed to be a sample of ^{235}U hexafluoride gas at a pressure of 1 Torr

at normal temperature ($3 \cdot 10^7$ nuclei in the laser focus volume). The numbers listed on the last line have been included for amusement. As indicated in the text, the inner electrons cannot contribute to the nuclear excitation.

Table IV. Maximum transfer probability per laser pulse from a storage level to a lasing state in ^{235}U . The characteristics of the laser beam are the following: photon energy $\hbar\omega = 5$ eV, flux $\phi = 7 \cdot 10^{16}$ W/cm, pulse duration 300 laser cycles ($\sim 2 \cdot 10^{-13}$ s). All electrons except those of the 1s, 2s and 2p shells have been assumed to participate to the nuclear excitation.

Table I.

$n\ell j$	$g^{n\ell j}$	K_ℓ	$\epsilon^{n\ell j}$ (keV) Ref. 8	$0^{n\ell j}(R_N)$ Ref. 9	$\langle r^{-2} \rangle^{n\ell j}$ (in a_0^{-2}) Ref. 10	$E^{n\ell j}$
1s1/2	2	1	-115.6	2.8 (-5)	2.44	4.8 (-8)
2s1/2	2	1	-21.77	4.8 (-6)	3.42	6.7 (-8)
2p1/2	2	1	-20.95	5.4 (-7)	3.27	6.4 (-8)
2p3/2	4	1	-17.17	---	1.12	2.2 (-8)
3s1/2	2	1	-5.58	1.1 (-6)	3.43	6.7 (-8)
3p1/2	2	1	-5.20	1.5 (-7)	3.39	6.6 (-8)
3p3/2	4	1	-4.32	---	1.19	2.3 (-8)
3d3/2	4	1	-3.73	---	1.15	2.3 (-8)
3d5/2	6	1	-3.56	---	1.02	2.0 (-8)
4s1/2	2	1	-1.46	3.2 (-7)	3.40	6.7 (-8)
4p1/2	2	1	-1.29	4.0 (-8)	3.33	6.5 (-8)
4p3/2	4	1	-1.06	---	1.19	2.3 (-8)
4d3/2	4	1	-.790	---	1.15	2.3 (-8)
4d5/2	6	1	-.748	---	1.02	2.0 (-8)
4f5/2	6	1	-.396	---	.999	2.0 (-8)
4f7/2	8	1	-.385	---	.962	1.9 (-8)
5s1/2	2	1	-.334	8.2 (-8)	3.39	6.6 (-8)
5p1/2	2	1	-.267	9.7 (-9)	3.23	6.3 (-8)
5p3/2	4	1	-.212	---	1.18	2.3 (-8)
5d3/2	4	1	-.113	---	1.13	2.2 (-8)
5d5/2	6	1	-.102	---	.998	2.0 (-8)
6s1/2	2	1	-.055	1.7 (-8)	3.65	7.2 (-8)
6p1/2	2	1	-.035	1.7 (-9)	3.39	6.6 (-8)
6p3/2	4	1	-.024	---	1.18	2.3 (-8)
5f5/2	3	7	-.0063	---	.858	1.2 (-7)
7s1/2	2	1	-.0052	1.8 (-9)	4.02	7.9 (-8)
6d3/2	1	5	-.0049	---	.923	9.0 (-8)

Table II.

$M\omega_N$ (eV)	$M\omega_0$ (eV)	λ	$\rho^{\text{Max}}(T_0, r_{\perp} = R_N)$		$P(T_0)$ all electrons		$P(T_0)$ two 3s elect.		$P(T_0)$ all except 1s, 2s		$P(T_0)$ all except 1s 2s 2p	
20	5	1	.38	10^{-1}	3.1	10^{-6}	9.8	10^{-8}	6.0	10^{-7}	5.3	10^{-7}
		2	.28	10^{-2}	2.1	10^{-7}	6.8	10^{-9}	2.5	10^{-8}	2.1	10^{-8}
		3	.54	10^{-3}	4.0	10^{-8}	1.3	10^{-9}	4.2	10^{-9}	3.4	10^{-9}
75	5	1	.37	10^{-1}	3.0	10^{-6}	9.6	10^{-8}	5.9	10^{-7}	5.2	10^{-7}
		2	.38	10^{-2}	2.1	10^{-7}	6.8	10^{-9}	2.5	10^{-8}	2.1	10^{-8}
		3	.54	10^{-3}	4.0	10^{-8}	1.3	10^{-9}	4.2	10^{-9}	3.4	10^{-9}
	3	1	.12	10^{-1}	9.8	10^{-7}	3.1	10^{-8}	1.9	10^{-7}	1.7	10^{-7}
		2	.93	10^{-3}	6.9	10^{-8}	2.2	10^{-9}	8.1	10^{-9}	6.7	10^{-9}
		3	.18	10^{-3}	1.3	10^{-8}	4.3	10^{-10}	1.4	10^{-9}	1.1	10^{-9}
	1.5	1	.30	10^{-2}	2.5	10^{-7}	7.8	10^{-9}	4.8	10^{-8}	4.2	10^{-8}
		2	.23	10^{-3}	1.7	10^{-8}	5.5	10^{-10}	2.0	10^{-9}	1.7	10^{-9}
		3	.44	10^{-4}	3.2	10^{-9}	1.1	10^{-10}	3.4	10^{-10}	2.8	10^{-10}
200	5	1	.42	10^{-1}	3.4	10^{-6}	1.1	10^{-7}	6.7	10^{-7}	5.8	10^{-7}
		2	.35	10^{-2}	2.6	10^{-7}	8.3	10^{-9}	3.0	10^{-8}	2.5	10^{-8}
		3	.66	10^{-3}	4.8	10^{-8}	1.6	10^{-9}	5.1	10^{-9}	4.2	10^{-9}
10^5	5	1	.40	10^{-1}	3.2	10^{-6}	1.0	10^{-7}	6.3	10^{-7}	5.5	10^{-7}
		2	.32	10^{-2}	2.4	10^{-7}	7.8	10^{-9}	2.8	10^{-8}	2.4	10^{-8}
		3	.61	10^{-3}	4.5	10^{-8}	1.5	10^{-9}	4.7	10^{-9}	3.9	10^{-9}
5 10^5	5	1	.38	10^{-1}	3.1	10^{-6}	9.8	10^{-8}	6.0	10^{-7}	5.3	10^{-7}
		2	.30	10^{-2}	2.2	10^{-7}	7.2	10^{-9}	2.6	10^{-8}	2.2	10^{-8}
		3	.58	10^{-3}	4.3	10^{-8}	1.4	10^{-9}	4.5	10^{-9}	3.7	10^{-9}

Table III.

^{235}U ELECTRONS TAKEN INTO ACCOUNT	NUCLEAR TRANSITION PROBABILITY PER CYCLE		NUMBER OF ISOMERS PRODUCED		
			during one laser cycle	during one pulse	in isomer lifetime
two 3s 1/2	1.3	10^{-9}	.04	11.7	~ 18,300
All except 1s, 2s, 2p	3.4	10^{-9}	.10	30.6	~ 47,700
All except 1s, 2s	4.2	10^{-9}	.13	37.8	~ 59,000
All	4.0	10^{-8}	1.2	360.	~ 560,000

Table IV.

TRANSITION MULTIPOLARITY λ	MAXIMUM TRANSFER PROBABILITY PER LASER PULSE ($B(E\lambda) = 1$ Weisskopf)	
1	1.7	10^{-4}
2	7.5	10^{-6}
3	1.3	10^{-6}

Table A-1: Numerical values of $C_{\lambda\mu}$ and analytical expressions of $P_{\lambda\mu}$, $f_{\lambda\mu}$ and $F_{\lambda\mu}$ for $1 \leq \lambda \leq 3$ and $0 \leq \mu \leq \lambda$.

λ	μ	$C_{\lambda\mu}$	$P_{\lambda\mu}(v)$ $\equiv (1 + v^2)^{\lambda+1/2} \times f_{\lambda\mu}(v)$	$(1 + u^2)^{\lambda-1/2} \times F_{\lambda\mu}(u)$
1	0	$(3/4\pi)^{1/2}$	v	-1
	1	$-(3/8\pi)^{1/2}$	1	u
2	0	$(5/16\pi)^{1/2}$	$2v^2 - 1$	-u
	1	$-(15/8\pi)^{1/2}$	v	-1/3
	2	$(15/32\pi)^{1/2}$	1	$u - 2u^3/3$
3	0	$(7/4\pi)^{1/2}$	$v^3 - 3v/2$	$(1 - 2u^2)/6$
	1	$-(21/64\pi)^{1/2}$	$4v^2 - 1$	-u
	2	$(105/32\pi)^{1/2}$	v	-1/5
	3	$-(35/64\pi)^{1/2}$	1	$u + 4/3 u^3 + 8/15 u^5$

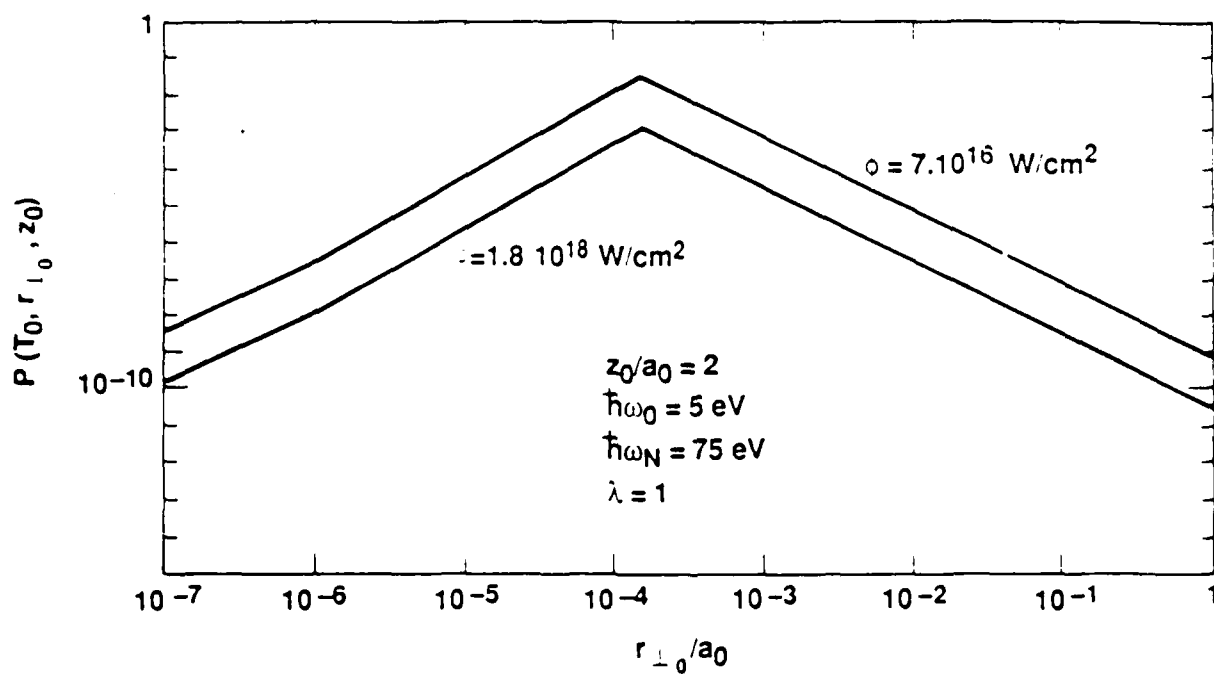


Fig. 1a

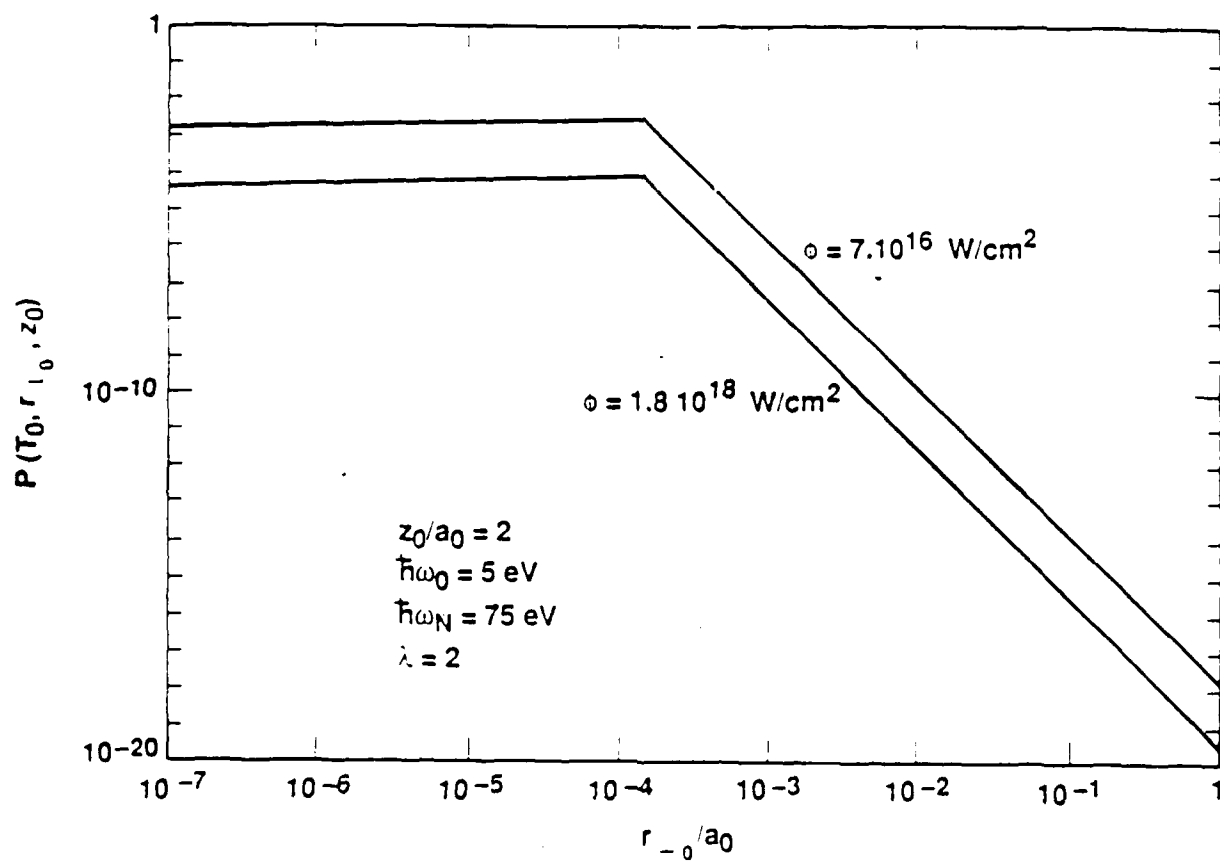


Fig. 1b

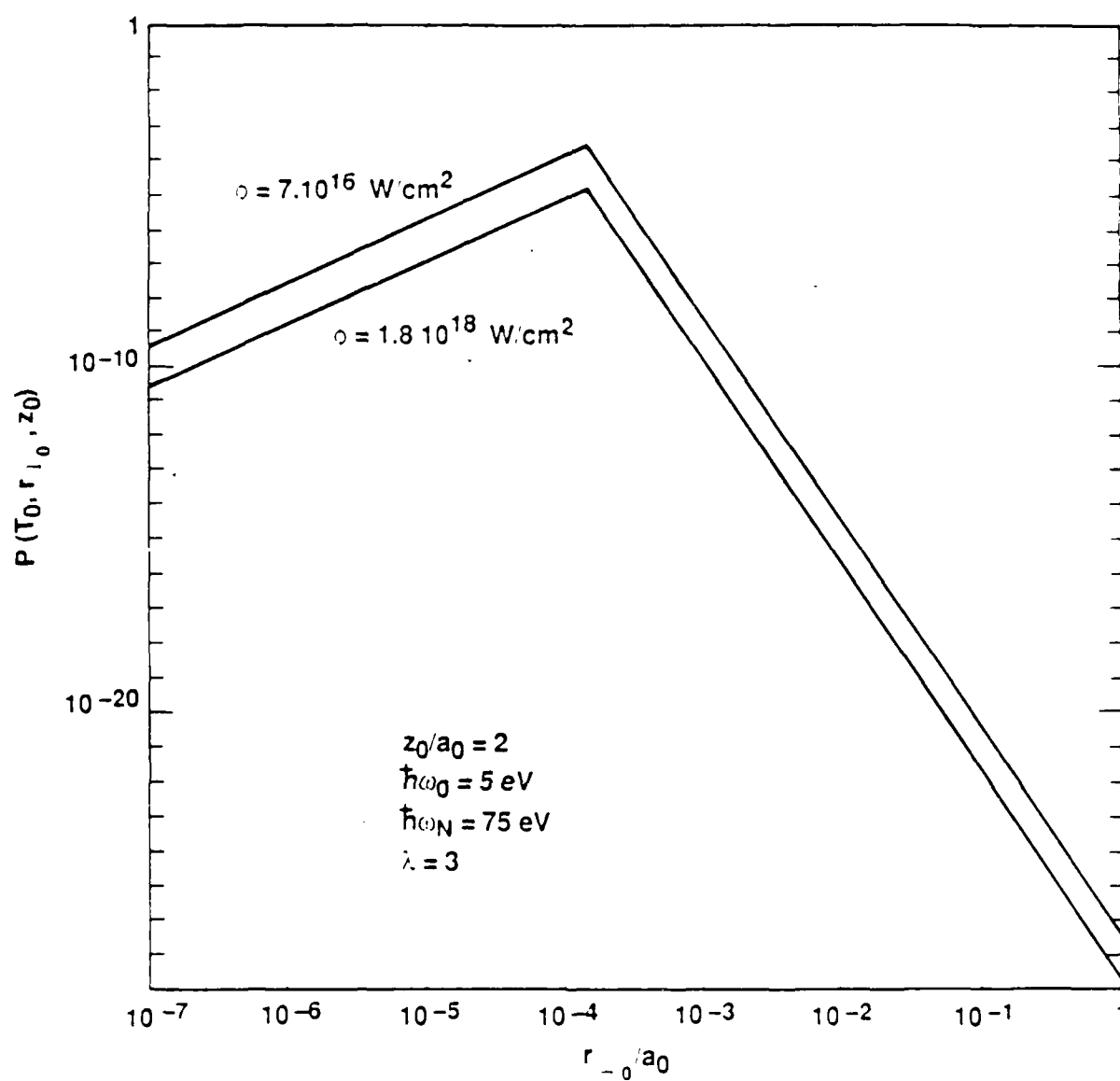


Fig. 1c

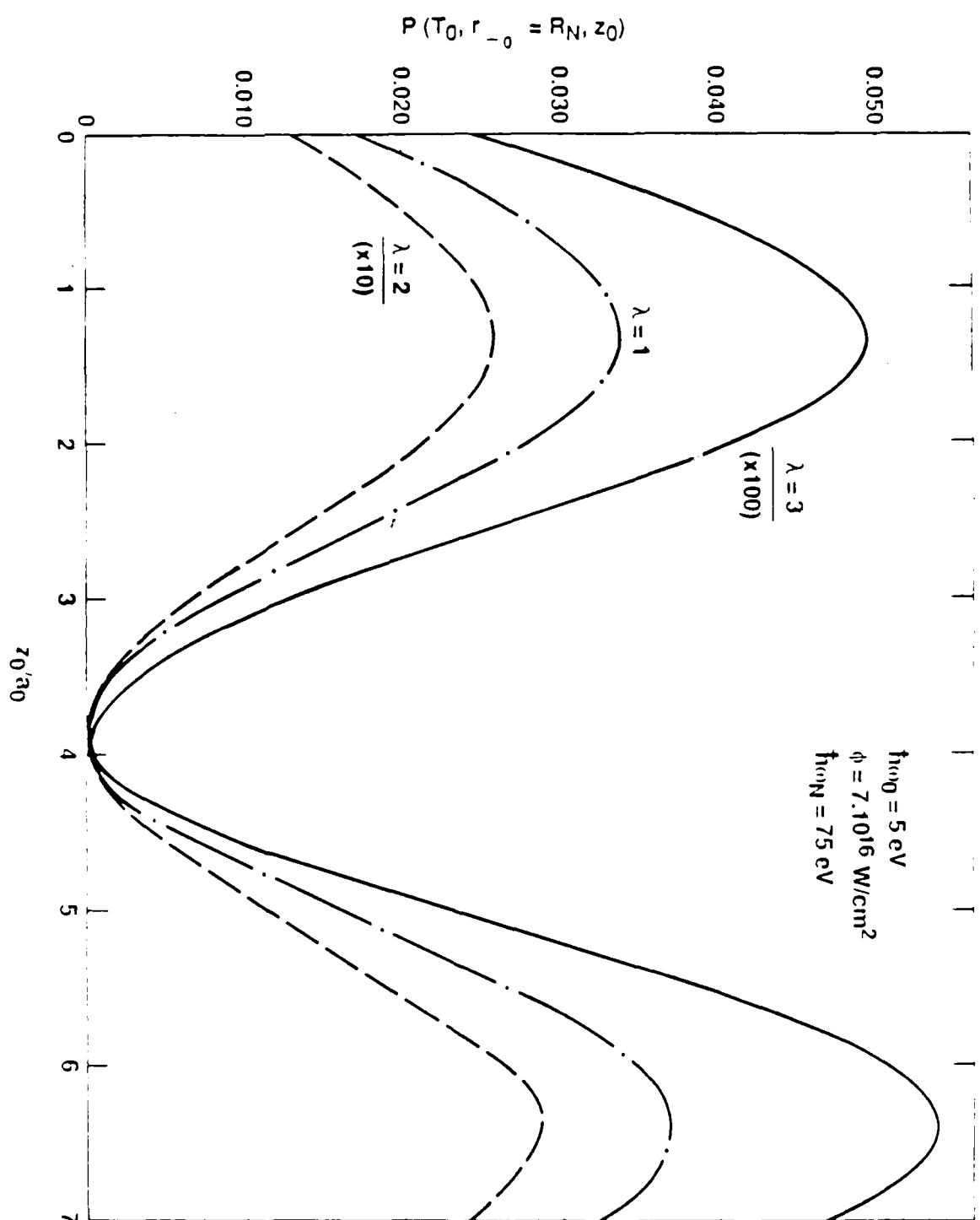


Fig. 2a

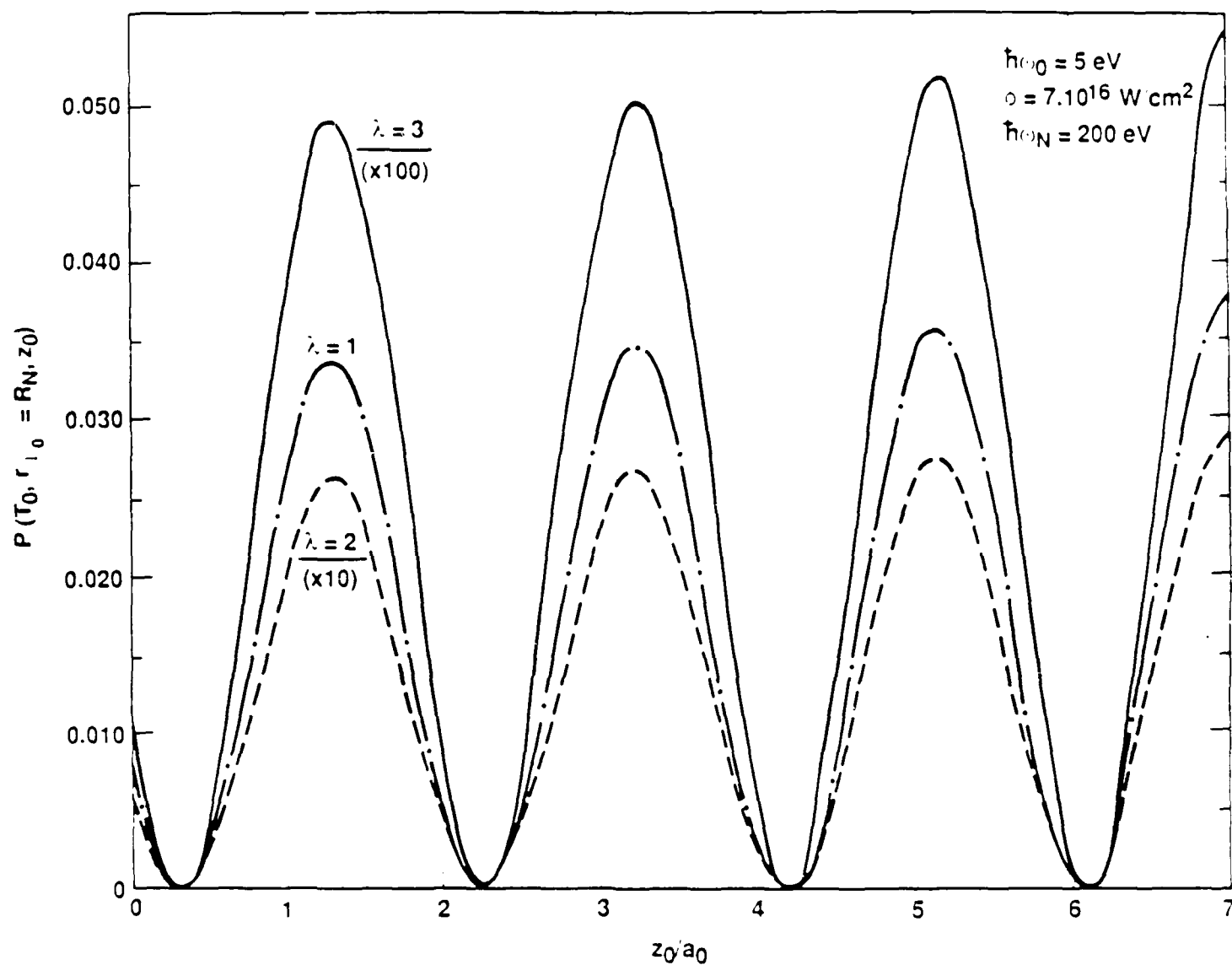


Fig. 2b

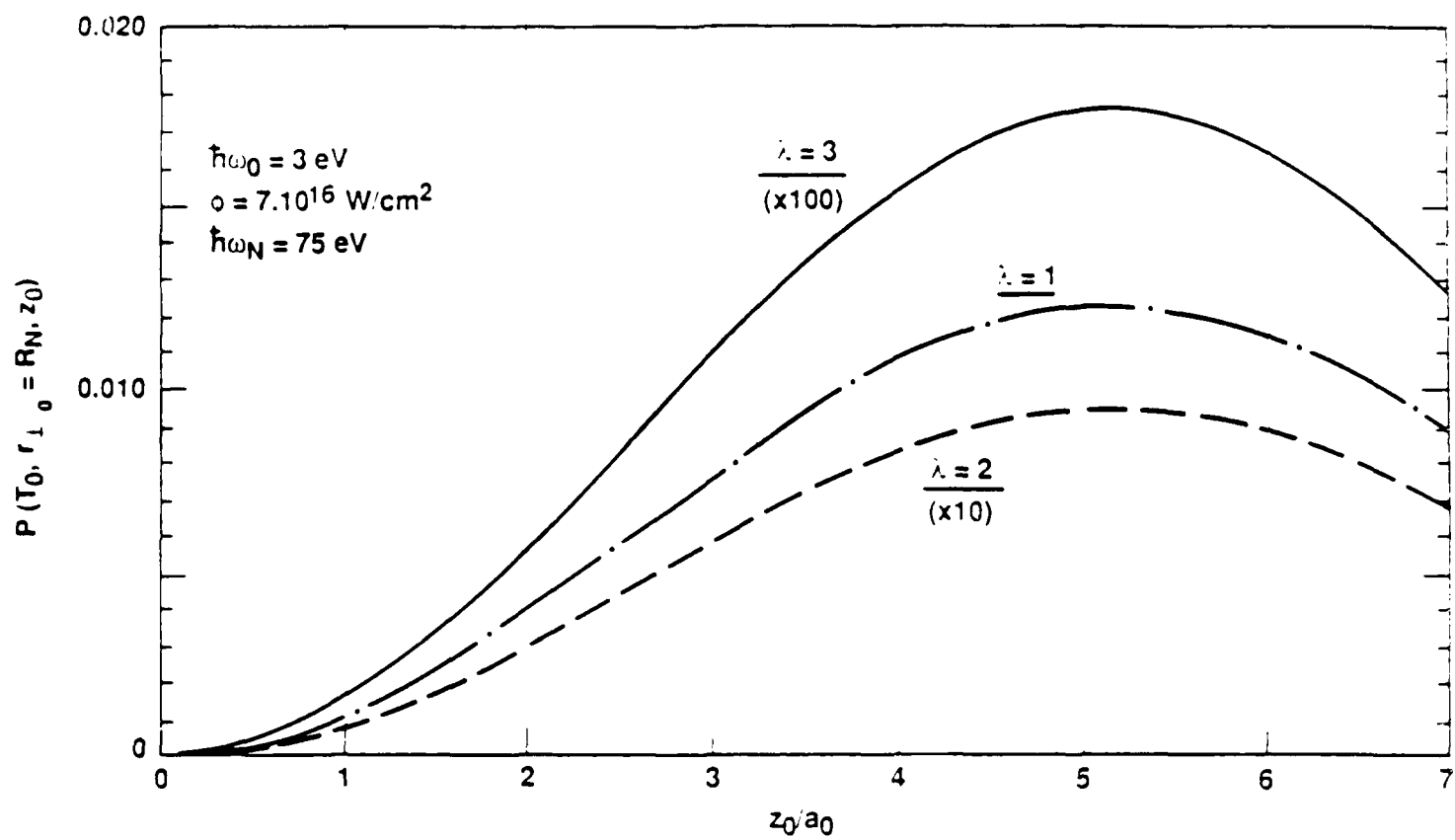


Fig. 2c

END

FEB.

1988

DTIC